Nature Environment and Pollution Technology
An International Quarterly Scientific Journal

p-ISSN: 0972-6268
(Print copies up to 2016)
e-ISSN: 2395-3454

Vol. 24 | No. S1 | pp. 1-18 | 2025

Original Research Paper

https://doi.org/10.46488/NEPT.2025.v24iS1.001

Open Access Journal

Design and Impact Analysis of a Grid-Connected Solar Photovoltaic System in Ibri, Oman

Arshad Mehmood† and Waleed Saif Abdullah Habib Al Kalbani
Department of Mechanical Engineering, College of Engineering, University of Buraimi, Al Buraimi 512, Oman
†Corresponding author: Arshad Mehmood; arshad.m@uob.edu.om

Nat. Env. & Poll. Tech.
Website: www.neptjournal.com

Received: 24-04-2024
Revised: 30-05-2024
Accepted: 02-06-2024

Key Words:
Solar energy
Photovoltaic system
Grid-connected
Economic analysis
Environmental impact

ABSTRACT

This study investigates the feasibility of establishing a grid-connected power system in Ibri, Oman. The primary goal is to address the rising energy demands and contribute to fighting climate change. By leveraging Ibri's resources, the research highlights the feasibility of such a system, focusing on its economic, technological, and environmental benefits. Using PVsyst software for planning and evaluation, the study assesses climate conditions, component choices, and performance predictions to ensure optimal system performance. The proposed 10.81 kWp solar power system estimates an energy production of 16,981 kWh, achieving a system efficiency of 67.2% based on the performance ratio (PR). The financial analysis estimates a payback period of 7.5 to 8.3 years, with an internal rate of return (IRR) of 11.15% and a net present value (NPV) of $32,024.28, confirming the project's viability. The system is expected to reduce carbon emissions by 379.939 tons over its lifetime, highlighting the significant ecological benefits of adopting solar energy (SE). The research demonstrates that incorporating PV systems in regions like Ibri is technically viable, economically beneficial, and environmentally advantageous. This study is a valuable resource for energy initiatives, promoting sustainable power production methods and encouraging the broader adoption of renewable technologies for a sustainable future.

INTRODUCTION

Solar energy (SE) is a sustainable option with the capacity to address the energy requirements of developing nations. Emphasizing its eco-friendly attributes, solar power has been identified as a critical avenue for achieving the IEA goal of net-zero emissions by 2050(Mukhopadhyay 2022). SE is seen as a vital contributor to enhancing energy efficiency and meeting growing energy demands (Bagwari et al. 2022). Despite its potential to mitigate greenhouse gas emissions, broader adoption is necessary to maximize its impact (Maran et al. 2022). SE's pivotal role extends beyond energy production to fostering development, job creation, and environmental preservation (Sheikholeslami 2023). There are two primary SE systems: PV and solar thermal. Solar PV systems convert light into electricity using cells and are considered a leading energy conversion method (Qingyang et al. 2021), while solar thermal captures heat for electricity generation and other uses (Shekhar 2018). Recent technological advances in solar cells and power electronics aim to boost the efficiency of solar PV generation (Nayak et al. 2022, Xu et al. 2023). The deployment of various solar configurations, including grid-tied, off-grid, large-scale, and building-integrated systems, demonstrates solar technology versatility and its contribution to reducing emissions and utilizing space effectively (Nayak et al. 2022). Solar PV systems have a notable lifespan, maintaining operational viability for up to 30 years, and are lauded for their ease of access as a renewable source (Peters & Sinha 2021, Rahman et al. 2023). The reduction in carbon dioxide emissions by using PV modules is significant, with ongoing research to improve the reliability of PV technology through mechanical enhancements and the application of efficiency-boosting coatings (Alimi et al. 2022, Yamaguchi et al. 2022).

Oman is actively pursuing SE, with investments in solar farms and an aim to increase wind production(Charabi 2023, Emerald Insight 2022, Ninzo et al. 2023). The country's solar radiation varies seasonally, reaching its zenith in June and ebbing in December (Zurigat et al. 2007), with year-round potential for solar power generation (Gastli & Charabi 2010, Tabook & Khan 2021). Innovative site selection for PV systems employs a variety of methodologies, including fuzzy analytical processes and integrated approaches that consider environmental and economic factors, supported by tools like GIS and BIM (Guo et al. 2021, Lee et al. 2015, Yousefi et al. 2018). Oman's commitment to sustainability is evident in its ambition to source 30% of electricity from

renewables by 2030 and the national oil company's strategy to shift a significant portion of its power usage to renewable sources (Al-Badi et al. 2009, Coyle 2017). This study assesses the deployment of a 10.8 kWp grid-connected solar PV system in Ibri, Oman, harnessing the area's high solar irradiance. Utilizing PVsyst software, the research aims to optimize the plant design and performance, factoring in local environmental conditions for enhanced efficiency. Covering a literature review, case study analysis, and system design optimization, the study evaluates both technical and economic feasibility, including environmental impact. The findings suggest Ibri's potential for advancing energy self-sufficiency and sustainable development, offering strategies for efficient solar PV usage that can inform renewable energy practices and aid Oman's renewable energy goals.

MATERIALS AND METHODS

Site Information

The design of a 10.81 KWp grid-connected solar PV system for a residential building in Ad Dubayshi, Ibri, Oman (23.1186°N, 56.4872°E). Using PVsyst software for optimization, the system, covering a roof area of 127 m² out of the available 1485 m², provides a stable and cost-effective energy solution as shown in Fig. 1. The configuration allows for surplus energy to be fed back to the grid, enhancing sustainability and offering financial incentives without the need for battery storage, suitable for both urban and remote applications.

Theoretical Background

PV systems transform sunlight into electricity by utilizing solar cells composed of semiconductor materials. These cells consist of layers of p-type and n-type semiconductors that possess different electrical properties; the p-type is abundant in positively charged holes, whereas the n-type is rich in electrons. At the junction of these layers, a depletion layer forms where charge carriers are sparse, creating an electric field as present in Fig. 2. This field is crucial for directing the movement of electrons to the n-type layer and holes to the p-type layer. When sunlight is absorbed by the semiconductor, photons energize the electrons, freeing them to move. This motion of electrons and holes under the influence of the electric field generates a flow of electricity and establishes a voltage across the cell. Connecting the solar cell to an external circuit allows this electricity to power devices, effectively converting SE into usable electric power.

System Overview and Components

The SPV system comprises elements such, as PV panels, batteries, inverters, charge controllers, cables the utility grid,

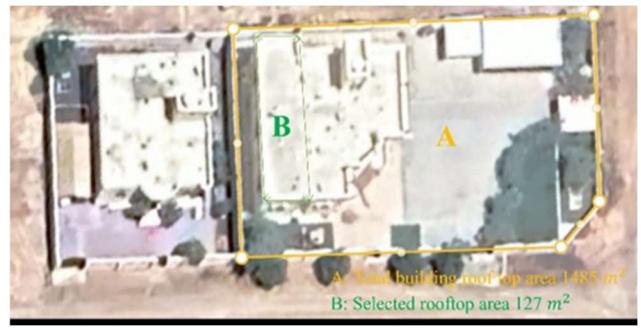

Fig. 1: Satellite view of the targeted location at coordinates 23.1186°N, 56.4872°E.

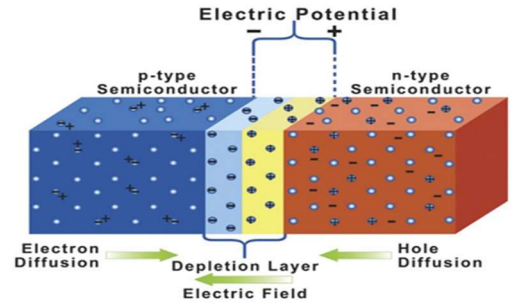

Fig. 2: Simplified version of solar cell.

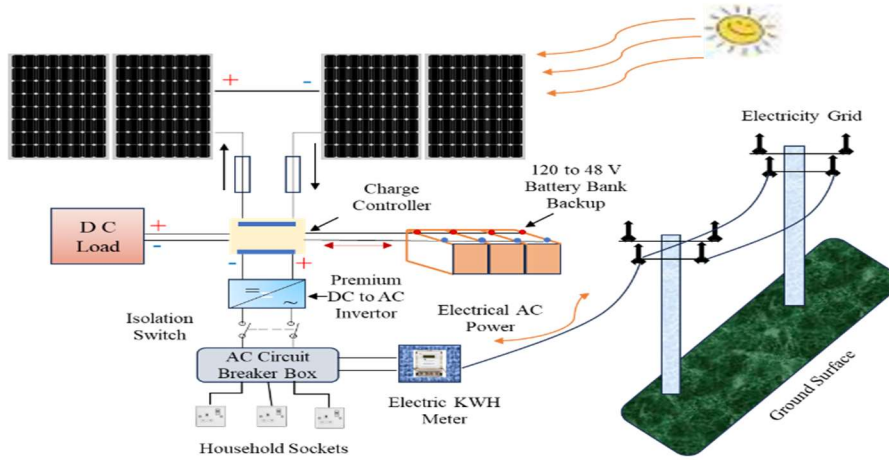

Fig. 3: A schematic representation of a solar power system connecting to the electricity grid and household sockets.

net metering, and loads as illustrated in Fig. 3. The direct current power produced by PV modules.

PV Arrays Selection

To achieve results, in this research we have tested monocrystalline solar panel models to select the most suitable PV array for different requirements, from the 'Trinca Solar' brand. Maximizing the efficiency of grid-connected PV systems involves critical components like PV arrays and inverters, analyzed using PVsyst software. This simulation, illustrated in a current-voltage (I-V) curve, demonstrates how a PV module's current and voltage respond to varying solar irradiance levels, from 200 W/m^2 to 1000 W/m^2 as depicted in Fig. 4. The curve highlights the MPP, where current and voltage multiply to yield the highest power output, decreasing as irradiance diminishes. Notably, the typical operating temperature for PV cells is 45°C, affecting performance as temperature rises. The study examines different Si-Mono PV modules under maximal solar radiation of 1000 W/m^2, showing varying power outputs:

- TSM-DD05H-08-(II)-295 generates 273.5 W with a current of 9.12 A and a voltage of 32.4 V.
- TSM-DD05H-08-(II)-305 produces 283.3 W, with a current of 9.25 A and a voltage of 33.1 V.
- TSM-DD05H-08-(II)-315 offers 292 W, with a current of 9.43 A and a voltage of 33.4 V.
- TSM-325DD14A(II) yields 299.9 W, with a current of 8.69 A and a voltage of 37.4 V.
- TSM-325DD14A(II) at 335 Wp outputs 308.9 W, with a current of 8.87 A and a voltage of 37.8 V.

This analysis underscores the influence of solar irradiance and temperature on the performance of PV modules, guiding optimal system configuration for enhanced SE utilization.

Solar Inverter

The K-solar KSY-11K on-grid solar inverter is selected for its high efficiency and performance, with a maximum efficiency of 98.20% and a EURO efficiency of 97.50%. It offers a nominal AC power output of 10.5 kW and supports a maximum DC input voltage of 1000 V, with dual MPPT inputs for optimal solar power generation from various PV array orientations as shown in Fig 5 (a, b). This transformerless inverter is lightweight and efficient, capable of delivering its full-rated power up to an ambient temperature of 45°C, with output power derating at higher temperatures. Designed for compatibility with 400 V grid systems and configurable for 50 Hz or 60 Hz, it is ideal for international applications. Featuring power factor correction to minimize reactive power charges, the inverter operates with zero power consumption at night. Suited for commercial installations, it offers robustness and versatility across different on-grid PV system configurations.

Solar Orientation Analysis

The solar orientation analysis, including tilt and azimuth angles, plays a vital role in optimizing solar panel placement for maximum energy absorption. The angle (α), ideally set to match the location's latitude, is determined to be 25° for this installation, closely aligning with the geographic latitude of 23°. The azimuth angle, crucial for directing the panels towards the sun, is measured in degrees from north (0°), with optimal solar exposure achieved when panels face true south (180°) in the Northern Hemisphere. This orientation ensures the panels capture the maximum sunlight, as direct north orientation would significantly reduce sunlight capture. Additionally, albedo, which reflects the earth's surface's ability to reflect sunlight, varies by location and surface texture. For this specific site, an albedo value of 0.2 is used,

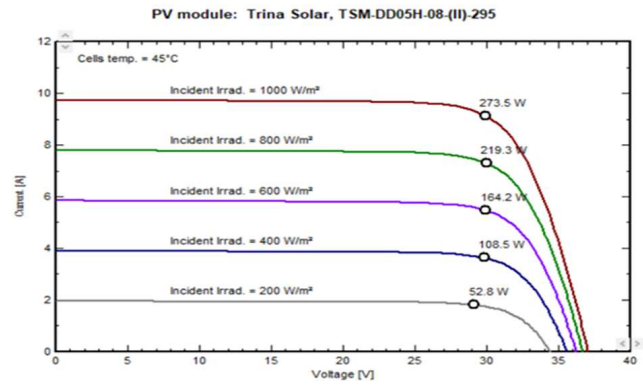

(a)

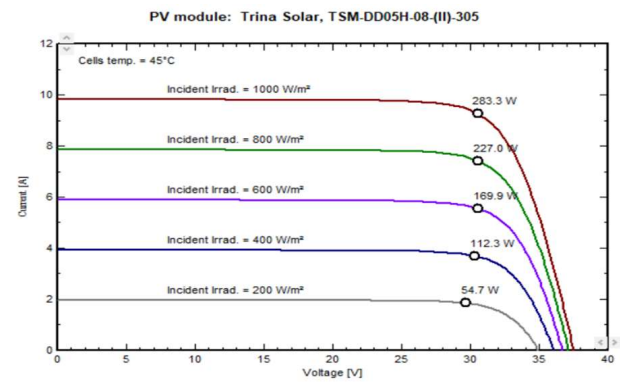

(b)

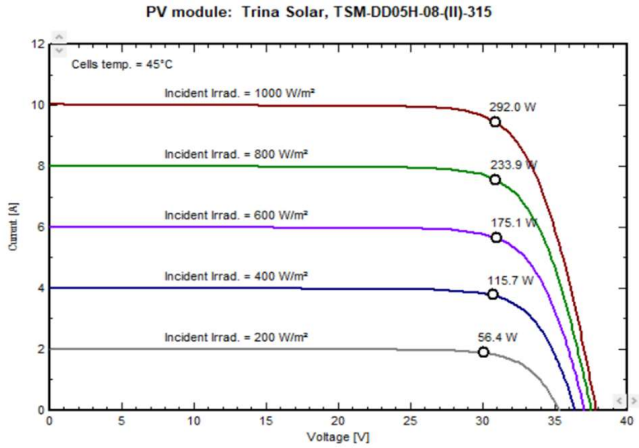

(c)

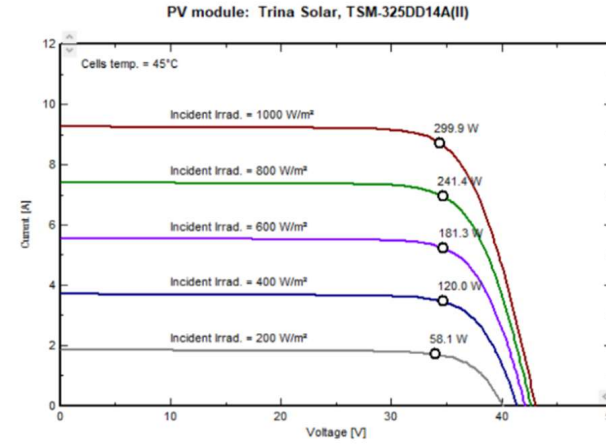

(d)

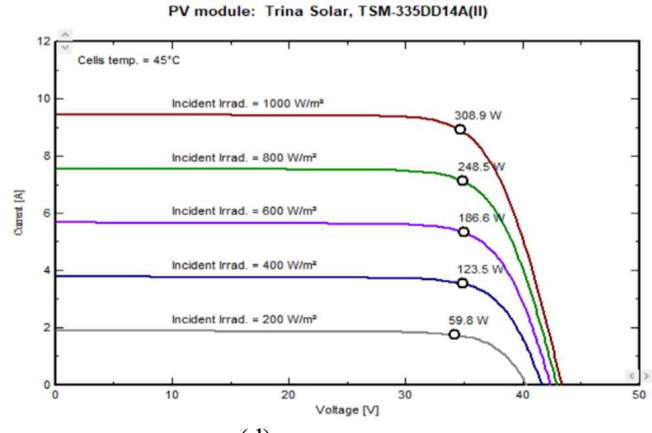

(d)

Fig. 4: The characteristics of irradiation effect by PV Si-Mono, (a) 295 Wp, 27 V; (b) 305 Wp, 27 V; (c) 315 Wp, 28 V; (d) 325 Wp, 32 V; and (e) 335 Wp, 32 V.

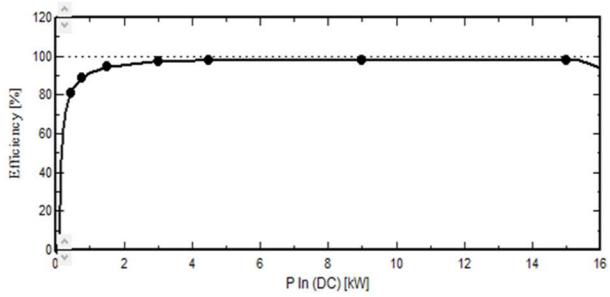

Fig. 5 (a): Efficiency vs input power curve of inverter.

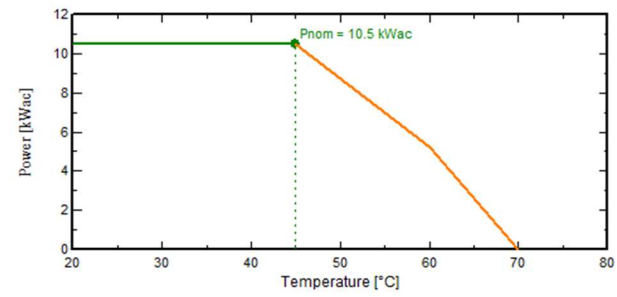

Fig. 5 (b): Power output vs temperature curve of inverter.

indicating moderate reflectivity. Adjusting both tilt and azimuth angles according to these principles is essential for enhancing the solar power system's efficiency and output.

Climatic and Geographic Resource

Fig. 6 is a sun path diagram for a specific location at Ad Dubayshi, with a latitude of 23.1886° N and a longitude of 56.4872° E, at an elevation of 333 meters. A sun path diagram is used to show the trajectory of the sun across the sky at different times of the day throughout the year. This particular diagram is set to local legal time. The curved lines represent the sun's path on given dates, marked by the numbered annotations (1 to 7), with the corresponding dates listed in the legend. These dates typically represent different times of the year, such as solstices and equinoxes, as well as points mid-way between them. For example, "1" marks the path on June 22nd, which is around the time of the summer solstice when the sun is highest in the sky. The concentric circles indicate the sun's altitude above the horizon in degrees, and the radial lines show the azimuth in degrees, where 0° is true north, 90° is east, 180° is south, and 270° is west. The shaded area signifies the periods during which the sun is above the horizon, that is, daytime. As the sun's elevation changes throughout the day, its position moves along a particular path corresponding to the date. The time of day is indicated by the curved lines that intersect the sun paths, labeled with hour markers (from 6 am to 6 pm in this case).

Our region utilizes Meteonorm to analyze the climatic conditions. PVSyst provides weather data, including wind speed, temperature, global horizontal irradiation, and diffuse horizontal irradiation. Table 1 elaborates, on the outcomes derived from Meteonorms weather assessments.

Numerical Simulation using PVSyst

PVsyst software is a sophisticated, user-friendly tool for designing and simulating PV systems, ideal for professionals and researchers. It features an intuitive interface, and a comprehensive meteorological database, and allows for manual data input for tailored analysis. Detailed reports with graphs and tables analyze various performance metrics, optimizing PV system performance.

Site Assessment for PV

The site assessment for a PV system in Ibri, Oman, based on data from 2021 to 2023 includes three key factors: solar

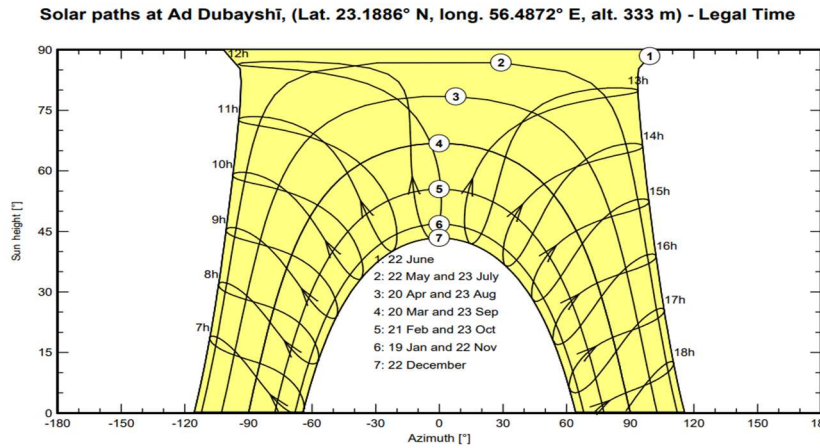

Fig. 6: Sun path diagram.

Table 1: Monthly weather from Meteonorm.

	Global horizontal irradiation	Horizontal diffuse irradiation	Temperature	Wind velocity	Linke turbidity	Relative humidity
	kWh/m^2/mth	kWh/m^2/mth	°C	m/s	[-]	%
January	140.6	35.4	18.0	2.90	4.061	58.1
February	146.4	47.5	20.3	3.30	5.036	48.0
March	178.5	74.4	24.4	3.49	6.338	37.1
April	203.7	76.4	29.0	3.40	7.000	29.2
May	216.1	91.0	34.1	3.31	7.000	23.1
June	206.3	100.0	35.7	3.40	7.000	27.1
July	199.6	104.5	37.3	3.60	7.000	29.5
August	188.4	103.6	37.0	3.49	7.000	29.9
September	181.9	77.0	34.0	3.29	7.000	32.4
October	170.2	57.4	30.5	3.00	5.261	34.1
November	147.2	34.7	24.4	2.80	4.199	48.7
December	133.1	36.1	20.0	2.70	3.951	57.1
Year	2112.0	838.0	28.7	3.2	5.904	37.9

Global horizontal irradiation year to year variability 6.1%

radiation, clearness index, and temperature. Despite high solar radiation peaking in May and June, the clearness index dips during these months due to atmospheric conditions like dust, impacting the effectiveness of radiation reaching the ground. Higher temperatures in these months could also reduce PV module efficiency. Overall, while high radiation suggests good electricity generation potential, variable clearness and high temperatures could affect overall system performance as presented in Fig. 7 (a, b). Decision-making for PV installation must consider these environmental factors along with economic and physical aspects.

Case Study

The plant has been designed by analyzing the daily electricity usage of a residential building located in Ibri Oman. To ensure a continuous supply put the loads data collection and load calculation are compulsory. The daily power demand can be calculated as follows from eq. 1 to eq. 4:

$$P_T = n \times P_R \quad \ldots(1)$$

$$E_T = h \times P_T \quad \ldots(2)$$

$$P_D = \sum E_T \quad \ldots(3)$$

$$E_g = 1.2 \times P_D \quad \ldots(4)$$

where, P_R is rated power, P_T is total power, E_T is total energy, P_D is power demand, E_g is gross energy, h is number of hours, and n is number of applications. The different appliances connected in residential buildings are given in Table 2 with their power ratings then the calculation is done for the total power and total energy based on h and n.

Performance Analysis

The analysis of the grid-connected PV system is conducted using specific parameters as recommended by the IEA. These parameters include: (Munshi 2023).

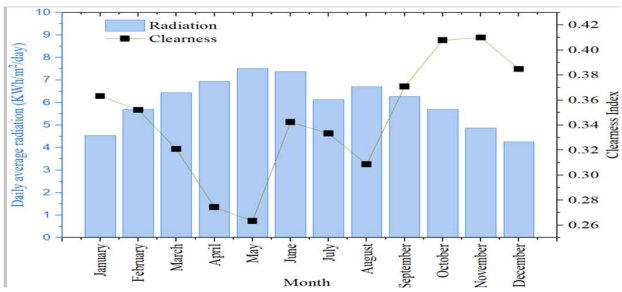

Fig. 7 (a): Global solar radiation and clearness.

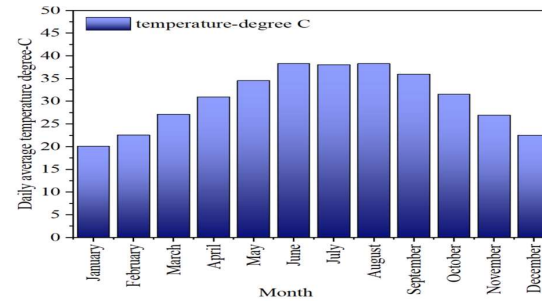

Fig. 7 (b): Average temperature yearly basis.

Table 2: Appliances used in a typical residential building.

Reference mark	Purpose	Rated power (KW)	n	Total power (KW)	Hour used h	Total energy (KWh / day)	Hours distribution
Room Air Conditioners	bedrooms and living areas	2	2	4	8	32	12 pm to 4 pm and 12 am to 4 am
Ventilation	maintaining air quality	0.1	1	0.1	24	2.4	All day
Dish and cloth washer	cleaning dishes and laundering clothes	1	1	1	2	2	12 pm to 2 pm
Refrigerator / Deep freezer	large unit	0.8	2	1.6/day	24	1.6	All day
Electric Stove /oven/Microwave	for cooking	3	1	3	6	18	9 am to 3 pm
Lighting	LED lighting	0.01	20	0.2	8	1.6	6 pm to 2 am
TV/PC/Mobile	entertainment	0.15	2	0.3	5	1.5	6 PM to 11PM
Stand by consumers	other useful household items	0.01	--	0.01	24	2.4	All day
Total Power				10.81		61.5	

Array Yield (Y_a): This represents the direct current (DC) energy generated by the solar photovoltaic (SPV) panel over a defined period (daily, monthly, or yearly) relative to its nominal power (rated capacity) at STC. It is quantified as:

$$Y_a = \frac{DC\ Energy\ Generated\ (DC\ voltage \times DC\ current \times time)}{Nominal\ Power\ at\ STC} \quad \ldots(5)$$

where DC energy is expressed in kWh and nominal power in kWp.

Reference Yield (Y_r): This metric assesses the efficiency of solar irradiation capture by comparing total horizontal solar irradiance to the global irradiance at STC, yielding an equivalent number of hours at global irradiance:

$$Y_r = \frac{Total\ Horizontal\ Irradiance}{Global\ Irradiance} \quad \ldots(6)$$

with total horizontal irradiance in kWh/m² and global irradiance in W/m².

Final System Yield (Y_f): This ratio indicates the total AC energy output from the inverter as a proportion of the rated SPV array power:

$$Y_f = \frac{AC\ Energy\ Output}{Peak\ Power} \quad \ldots(7)$$

Performance Ratio (PR): An essential measure of a PV system's operational efficiency, the PR compares the actual system output to its theoretical potential by dividing the final system yield by the reference yield:

$$PR = \frac{Final\ System\ Yield}{Reference\ Yield} \quad \ldots(8)$$

This ratio highlights system losses during DC to AC conversion, accounting for factors such as irradiation levels, panel temperature, and grid availability.

Capacity Utilization Factor: This evaluates the actual output of a PV plant against its maximum possible output:

$$Capacity\ Utilization\ Factor = \frac{Energy\ measured\ in\ KWh}{365 \times 24 \times Installed\ capacity\ of\ PV\ plant} \quad \ldots(9)$$

Inverter Efficiency: Defined as the ratio of AC output power to DC output power, reflecting the conversion efficiency of the inverter:

$$Inverter\ Efficiency = \frac{AC\ output\ power}{DC\ power} \quad \ldots(10)$$

System Efficiency: This is calculated by multiplying the PV module efficiency by the inverter efficiency.

Energy Output: The energy directed to the utility grid is monitored at the inverter's AC output terminals, both daily and monthly (Kim et al. 2023) .

Energy Losses: The overall efficiency and performance of a PV system are impacted by two primary types of losses:

System Losses (L_s): Resulting from inverter inefficiencies.

Array Capture Losses (L_c): Due to factors like shading, module mismatch, and soiling that affect the PV array's ability to capture and convert SE efficiently.

$$L_s = Y_a - Y_f \quad \ldots(11)$$

$$L_c = Y_r - Y_a \quad \ldots(12)$$

These comprehensive analyses provide critical insights into the performance and optimization potential of PV installations.

System Orientation

To get the right and optimal selection of Solar PV devices, simulations are performed with different solar PV device

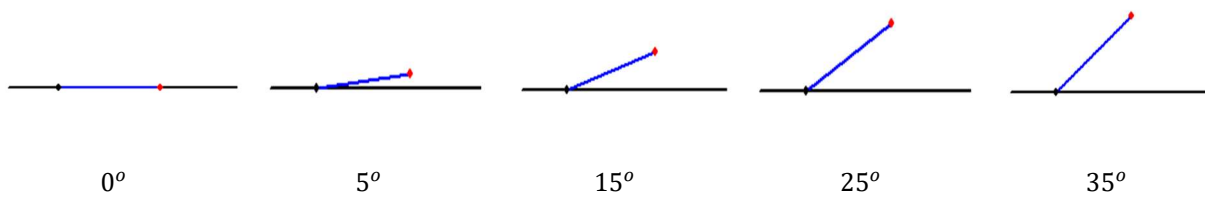

Fig. 8: Various tilt angles (α) used in simulation results for PV orientation at 0°, 5°, 15°, 25°, and 35°.

Table 3: Constant and variable in PVsyst simulation.

Selection	Parameter selection	Desired values
Constant	Longitude	E
	latitude	E
	Albedo	0.2
	Azimuth	0
	Invertor	10.5 KW
	System losses	Described in Table 3
Variable	Tilt Angle (annual basis)	, , 1, 2, 3
	PV system capacity	295, 305, 315, 325, 335

Table 4: Simulation results with PV module variants.

Simulation	PV orientation	PV					Invertor			
		Model	Capacity	No. of modules	Pnom total	Module Area	Capacity	No,	E_{array}	E_{grid}
1	Tilt 0	S- Mono (TSM-DEG5-II-295	295,27 V	38	11.21	61	10.5 Kw ac	1	16266	15887
2	Tilt5								16802	16417
3	Tilt 15								17549	17155
4	Tilt 25								17852	17453
5	Tilt 35								17705	17308
6	Tilt 0	S- Mono TSM-DD05H-08-(II)-305	305, 28V	36	10.98	58	10.5 Kw ac	1	16844	16458
7	Tilt5								17400	17007
8	Tilt 15								18175	17772
9	Tilt 25								18489	18082
10	Tilt 35								18337	17931
11	Tilt 0	S- Mono TSM-DD05H-08-(II)-315	315, 28V	38	11.97	57	10.5 Kw ac	1	17372	16979
12	Tilt5								17945	17545
13	Tilt 15								18745	18333
14	Tilt 25								19069	18653
15	Tilt 35								18912	18498
16	Tilt 0	Si-Mono TSM-325 DD14A (II)-325	325WP, 32V	34	11.05	64	10.5 Kw ac	1	16036	15660
17	Tilt5								16554	16172
18	Tilt 15								17272	16882
19	Tilt 25								17556	17161
20	Tilt 35								17408	17015
21	Tilt 0	Si-Mono TSM-325DD14A(II)-335	335WP, 32 V	32	10.72	62	10.5 Kw ac	1	16536	16154
22	Tilt5								17069	16680
23	Tilt 15								17809	17411
24	Tilt 25								18101	17699
25	Tilt 35								17949	17549

Table 5: Description of losses.

Loss Fraction	Measurement Unit	
Module Quality loss: The difference between PV module performance as specified by the manufacturer and actual performance	Loss Fraction	
	1.1 %	
Light-Induced Degradation Loss: decrease in efficiency that some solar panels experience when they are first exposed to sunlight.	Loss Fraction	
	2 %	
Soiling Losses: loss due to dust particles which gets accumulated on solar panels over time	Loss Fraction	
	3 %	
Series Diode Loss: Occurs due to the voltage drop across diodes which are used in solar panels to prevent reverse current flow.	Voltage drops	Loss Fraction
	0.7 V	0.1% at STC
Module Mismatch Loss: occurs when there is a variation in the performance of individual solar modules in an array, which can lead to less-than-optimal energy production.	Loss Fraction	
	2% at MPP	
Thermal Loss according to irradiance: Occurs due to the increase in cell temperature, which typically causes a decrease in PV module efficiency.	U_c (constant)	29.0 W/K
	U_n (wind)	0.0 W/K/m/s
String Mismatch Loss: occurs when there is a discrepancy in output between different strings of solar panels due to variations in shading, orientation, or panel degradation.	Loss Fraction	
	0.1 %	
DC Wiring Losses: due to the resistance in the DC cabling that connects the solar panels to the inverter, which can cause energy to be lost as heat.	Global array res.	Loss Fraction
	103 mW	1.5% of STC
Module average degradation: The annual percentage decrease in module performance over time is missing. Solar panels slowly degrade each year, reducing their output.	Years	Loss Factor
	10	0.4%/year
Mismatch due to degradation: Over time, modules degrade at different rates, which can increase mismatch losses.	Imp RMS Dispersion	Vmp RMS Dispersion
	0.4%/year	0.4%/year
IMA Loss Factor: possibly associated with installation and maintenance adjustments or inaccuracies in modeling versus actual performance.	ASHRAE Param: IMA	1-bo(1/cosi-1)
	Bo Param	0.05

models so that the results can be seen with different PV orientation variants 0°, 5°, 15°, *25°* and 35° shown in Fig. 8. These parameters are detailed in Table 3, which outlines the constant and variable parameters used in the PVsyst simulation. The results of these simulations, showcasing the performance of PV modules at varying orientations and capacities, are presented in Table 4**.**

System Losses

The proposed methodology is ensured for a 30-year lifespan for the selected site. During this period, many losses take place inside the system and become the main reasons for the malfunctioning of the mechanism. In this section various losses are described, to understand the quality of the system performance. These are explained below in Table 5.

RESULTS AND DISCUSSION

Summary of the PV System

The PV system simulation at Ad Dubayshi, using PVSyst 7.3 software without considering shading, utilized TSM-DD05H (II)-315 modules and a KSY-11K inverter oriented at 25 degrees. The annual energy output was 16,981 kWh with a specific yield of 1,419 kWh/kWp as shown in Fig. 9 (a). The PR was 0.672, factoring in losses detailed in the system and array efficiencies. Fig. 9 (b) illustrates a positive correlation between daily energy output (kWh/day) and global solar irradiance (kWh/m²/day), demonstrating typical variability in production influenced by meteorological conditions and solar angles over the year.

Balances and Main Results

The PVsyst software analysis presents detailed performance metrics for a PV system, including global horizontal irradiation at 2112.0 kWh/m²/year and incident irradiation on the collector plane at 2111.2 kWh/m²/year. Diffuse irradiation is measured at 837.8 kWh/m² with an average ambient temperature of 28.76°C. The PV array produces a total annual energy yield of 17,375 kWh, with 16,981 kWh delivered to the grid. The system's PR averages 67.2% annually, with grid injection ranging from 1,098 kWh in December to 1,710 kWh in May.

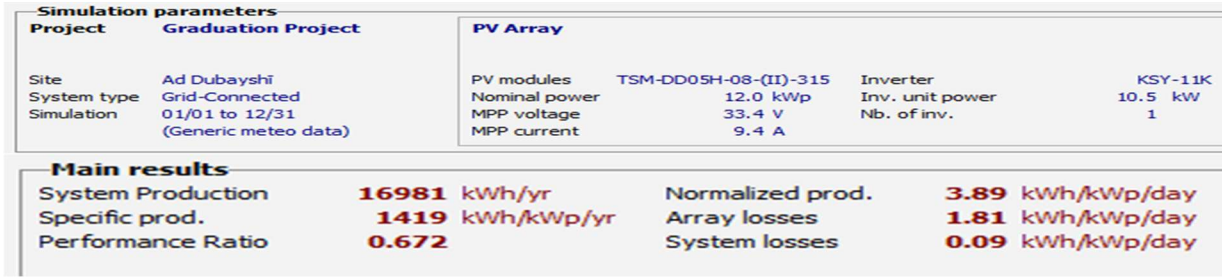

(a)

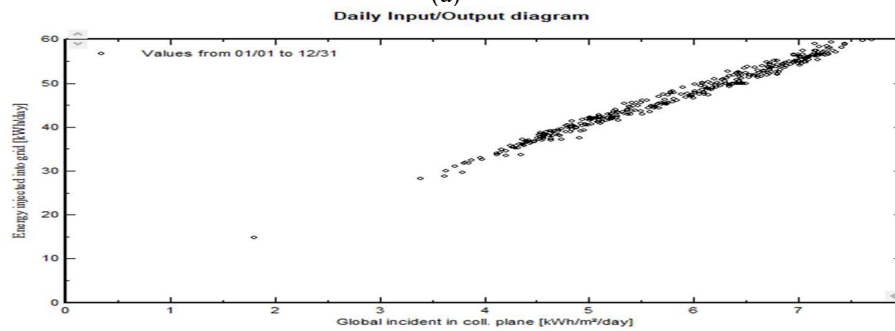

(b)

Fig. 9: Summary of the PV system (a) Annual performance data of a grid-connected PV system; (b) Daily PV energy output relative to solar irradiance.

Normalized Performance Coefficient and PR

The International Electrotechnical Commission (IEC) has set standardized metrics such as the normalized production coefficient and PR to benchmark PV system performance. Fig. 10 (a) in the report delineates the monthly normalized production, which is detailed in Table 6. Fig 10 (b) showcases the monthly PR. The reported normalized array losses, termed collection loss and denoted as Lc, are 1.81 kWh/kWp/day. Additionally, the normalized system losses, including

Table 6: Balances and main results.

Month	GlobHor kWh/m^2	DiffHor kWh/m^2	T_Amb °C	GlobInc kWh/m^2	GlobEff kWh/m^2	EArray kWh	E_Grid kWh	PR ratio
January	140.6	35.4	17.98	140.6	10.4	1206	1176	0.699
February	146.4	47.5	20.33	146.4	136.6	1247	1219	0.696
March	178.5	74.4	24.41	178.3	167.9	1502	1469	0.688
April	203.7	76.4	28.99	203.6	192.8	1682	1646	0.676
May	216.1	91.0	34.05	216.1	204.7	1749	1710	0.661
June	206.3	100.0	35.68	206.3	195.6	1660	1622	0.657
July	199.6	104.5	37.31	199.5	189.0	1596	1559	0.653
August	188.4	103.6	36.97	188.3	178.1	1509	1474	0.654
September	181.9	77.0	34.00	181.9	171.7	1475	1442	0.662
October	170.2	57.4	30.46	170.2	160.0	1398	1364	0.669
November	147.2	34.7	23.35	147.0	136.2	1227	1200	0.682
December	133.1	36.1	20.00	133.0	122.1	1124	1098	0.690
Year	2112.0	837.8	28.76	2111.2	1985.1	17375	16981	0.672

Legends

GlobHor	Global horizontal irradiation		
DiffHor	Horizontal diffuse irradiation	EArray	Effective energy at the output of the array
T_Amb	Ambient Temperature	E_Grid	Energy injected into the grid
GlobInc	Global incident in coll. plane	PR	Performance Ratio
GlobEff	Effective Global, corr. For IAM and shadings		

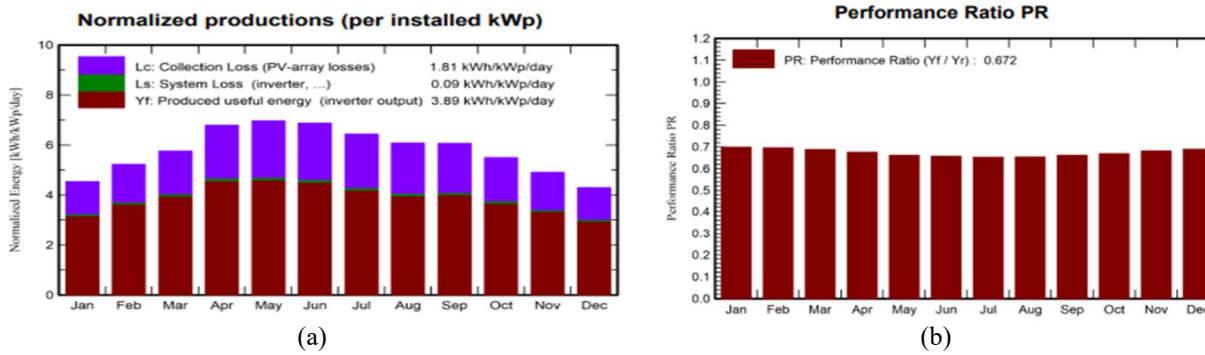

Fig. 10: (a) Monthly normalized energy production and losses; (b) Monthly PR of the PV system.

inverter losses labeled as Ls, stand at 0.09 kWh/kWp/day. The PV system's useful energy output is noted as 3.89 kWh/kWp/day. The graphical representation indicates monthly fluctuations in electricity production, with the highest in May and the lowest in December. Based on simulation results, the system's annual PR is calculated at 67.20%, as depicted in Fig 10.

PV Array Efficiency

Fig. 11 (a-e) displays the performance characteristics of the Trina Solar TSM-DD05H(II)-315 PV module under varying environmental conditions. These graphs include; Power-Voltage (P-V) Curves at Different Irradiances: Illustrates power output in watts across different voltage levels at various irradiances, with cell temperature held constant at 45°C. For example, at 1000 W/m² irradiance, maximum power output (Pmax) reaches 292.0 W, while at 200 W/m², it drops to 56.4 W. Current-Voltage (I-V) Curves at Different Temperatures: Depicts current output in amperes across voltage ranges at a constant 1000 W/m² irradiance, showing how output varies with temperature. Pmax values include 332.2 W at 10°C and 261.6 W at 70°C. Power-Voltage (P-V) Curves at Different Temperatures: Plots power output against voltage at 1000 W/m² irradiance across temperatures, showing a decrease in Pmax from 332.2 W at 10°C to 261.6 W at 70°C. Efficiency Curve Relative to STC: Details the module's efficiency relative to a standard irradiance of 1000 W/m², with an STC efficiency of 18.97%. Efficiency variations are tracked at lower irradiances, such as a 0.2% increase at 800 W/m² and a 3.0% decrease at 200 W/m². Efficiency Curve Relative to STC (Temperature Impact): Demonstrates efficiency declines as cell temperature increases, with efficiency starting around 18-20% at 25°C and decreasing to about 15-17% at 60°C under 1000 W/m² irradiance. These detailed analyses are critical for optimizing solar installations to maintain high efficiency under varying environmental conditions, allowing for system designs that adapt to temperature and irradiance changes effectively.

Solar PV System Performance and Irradiance Analysis

Fig. 12 (a), titled "System Output Power Distribution," illustrates the frequency distribution of power injected into the grid over a year. The X-axis, ranging from 0 to 8 kW, segments power into bins, with the Y-axis measuring occurrence frequency up to 600 classes (0.1 MWh each). The histogram peaks between 4 and 5 kW, marking the most common output range, with less frequent extremes on either end. Fig. 12 (b) details the distribution of solar irradiation, with the X-axis showing "Global incident in coll. plane [W/m²]" from 0 to 1200 W/m², and the Y-axis in classes of 0.01 MWh/m² up to 100 classes. Most solar power is received around 600 W/m². Fig. 12 (c) presents a "Daily System Output Energy" time series for a year, with daily values fluctuating up to 60 MWh, indicating a variable and dynamic system influenced by factors that cause significant day-to-day output variations.

Diagram of Energy Flow and Losses

Fig. 13, illustrates the energy flow and loss diagram for the PV system over the year. The global horizontal irradiation received on the collector plane is 2112 kWh/m², which is subject to a 3.07% IAM factor loss and a 3% soiling loss factor, resulting in an effective irradiation of 1985 kWh/m² on the collectors. The solar panels, with an efficiency of 18.97% at STC, convert this into a nominal energy output of 23782 kWh. The energy at the MPP is further reduced to 17375 kWh due to various losses, including a 9.79% module degradation over 25 years, losses due to irradiance and temperature, quality, and light-induced degradation (LID). Ohmic wiring loss contributes to a further 0.83% reduction. After accounting for the energy conversion efficiency of the inverter, the available energy at the inverter output totals 16981 kWh, which is the same amount of energy injected into the grid.

Comparative Analysis

The comparative analysis highlights the techno-economic viability of solar PV systems in Oman, focusing on

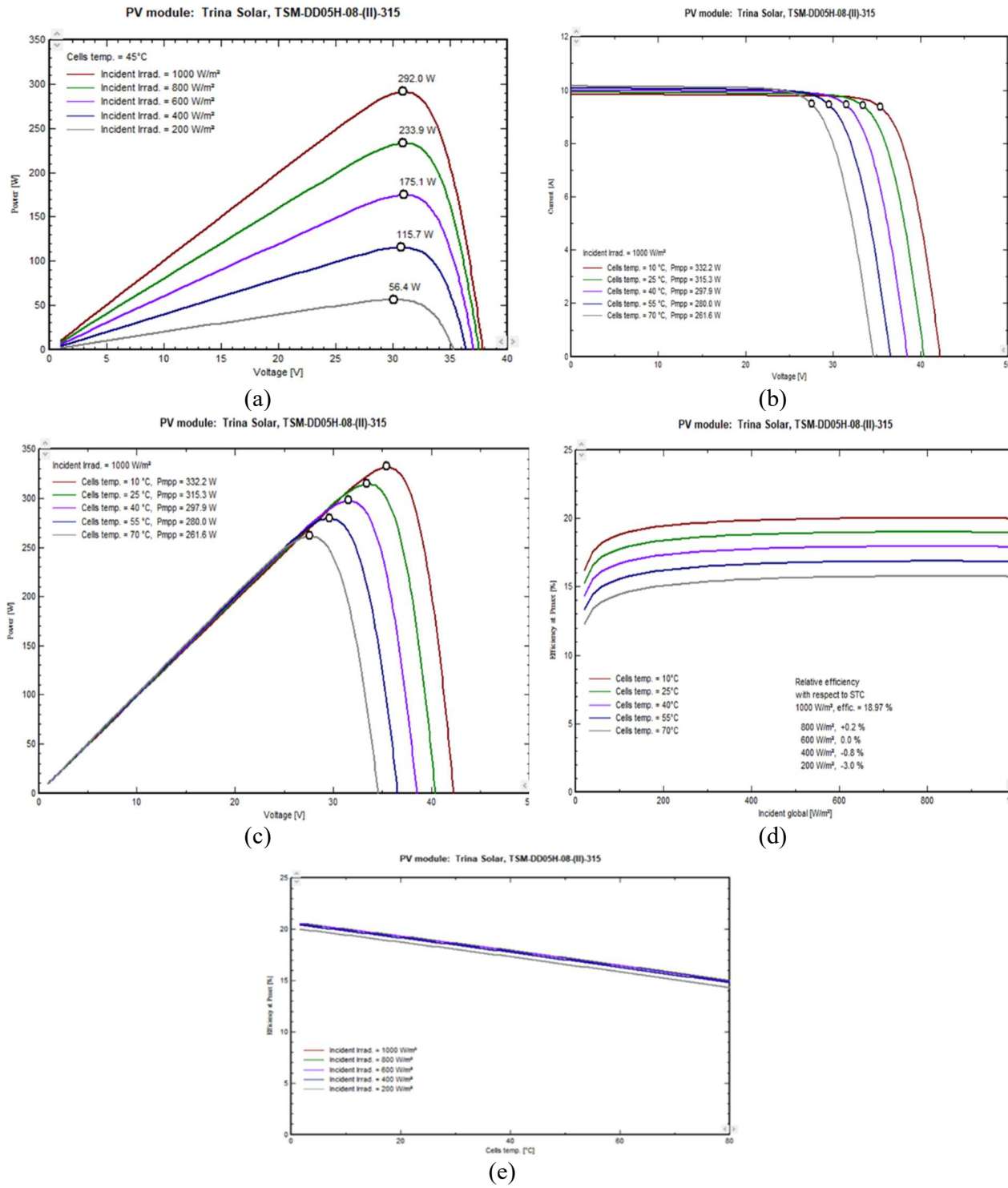

Fig. 11: (a) I-V characteristics of the PV module at various irradiance levels; (b) I-V curves of the PV module at different cell temperatures; (c) P-V curves at multiple irradiance levels for the PV module; (d) Efficiency variation of the PV module with changing irradiance; and (e) Derivative of I-V curve showing MPP tracking.

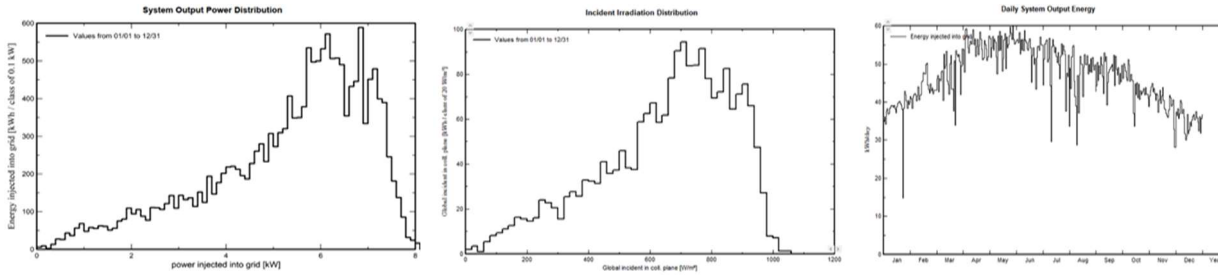

(a) (b) (c)

Fig. 12: (a) P_{max} – incident global production curve; (b) Incident irradiation distribution; (c) Daily energy injected into the grid.

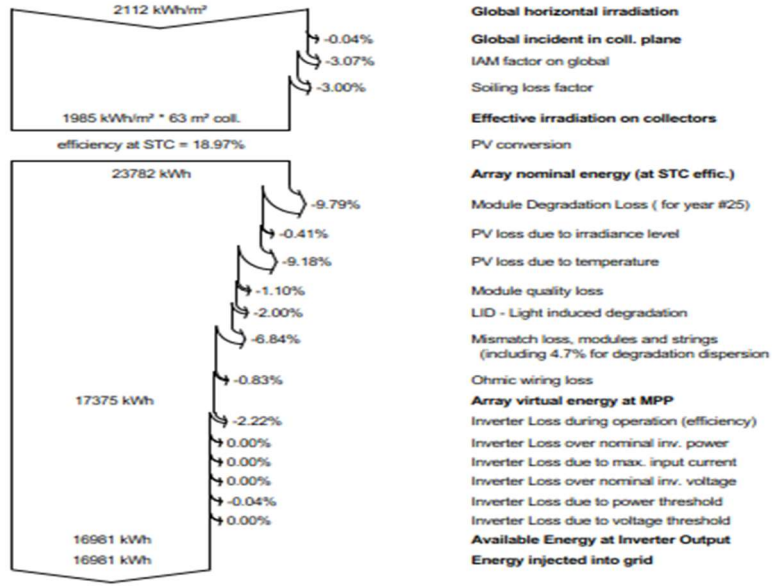

Fig. 13: Loss diagram.

feasibility, design, and economic dispatch. Key findings emphasize system efficiency, annual energy production, and payback periods, while limitations include a lack of detailed environmental analysis and focus on specific configurations, as given in Table 7.

Economic Analysis

An economic study was conducted to assess the initial capital cost and payback period for a PV installation, focusing on component costs. Costs were identified for Trinca solar modules at $195 each and Krylosar inverters at $1500 each

Table 7: Comparative analysis of solar PV system.

	Focus	Key findings	Limitations	Ref.
Techno-economic feasibility analysis of 1 MW photovoltaic grid-connected system in Oman	Feasibility analysis of 1 MW photovoltaic	Highlights the economic and technical viability of a 1 MW grid-connected system in Oman.	The study focuses on economic and technical aspects without detailed environmental analysis.	(Albadi et al. 2019)
Economic Dispatch of Oman's Main Interconnected System	Economic dispatch of the power system with a 500MW solar PV plant	Investigates economic dispatch strategies incorporating a large-scale solar PV plant.	Primarily focuses on economic dispatch without in-depth environmental impact.	(Kazem et al. 2017)
Feasibility, design, and impact analysis of a grid-connected solar PV system	Feasibility, design, and impact analysis of a grid-connected solar PV system	10.81 kWp system design, 16981 kWh annual energy production, 67.2% system efficiency, 7.5-8.3 years payback period, significant CO_2 reduction.	The study is limited to a specific location and system configuration.	Present study

Table 8: Initial investment costs and annual operating expenses for PV system.

Investment and charges

Description	Quantity	Unit price	Total	
PV modules			9,120.00	USD
TSM-DD05H-08-(II)-315	38.00	195.00	7,410.00	USD
Supports for modules	38.00	45.00	1,710.00	USD
Inverters			1,500.00	USD
KSY-11K	1.00	1,500.00	1,500.00	USD
Other components			1,600.00	USD
Accessories, fasteners	1.00	450.00	450.00	USD
Wiring	1.00	920.00	920.00	USD
Combiner box	1.00	230.00	230.00	USD
Studies and analysis			0.00	USD
Installation			3,800.00	USD
Global installation cost per ...	38.00	100.00	3,800.00	USD
Insurance			0.00	USD
Land costs			0.00	USD
Loan bank charges	0.00	0.00	0.00	USD
Taxes			0.00	USD
		Total installation cost	**16,020.00**	**USD**
		Depreciable asset	11,070.00	USD

Operating cost (yearly)

Description	Yearly cost	
Maintenance	1,040.00	USD
Provision for inverter re...	210.00	USD
Salaries	470.00	USD
Repairs	260.00	USD
Cleaning	100.00	USD
Security fund	0.00	USD
Land rent	0.00	USD
Insurance	0.00	USD
Bank charges	0.00	USD
Administrative, accounti...	0.00	USD
Taxes	0.00	USD
Subsidies -	0.00	USD
Operating costs (OPEX)	**1,040.00**	**USD/year**

[solar panel, solar inverter], as outlined in Table 8. Costs for studies, analysis, insurance, land, loans, and taxes were excluded from this assessment, with maintenance costs estimated from other studies.

Financial parameter: Fig. 14 appears to be a financial model for this project with a 25-year lifespan starting in 2025. It assumes no inflation or production variation over time, no income tax, and includes a tax depreciation section for assets like PV modules and inverters. Financing is set at $16,020, all from own funds as depicted by the pie chart, indicating no loans or subsidies are involved. The total redeemable amount is $11,070.

Electricity sale on availability and demand: Fig. 15 shows settings for an energy pricing model with a variable tariff structure. It includes an hourly peak/off-peak tariff, feed-in tariffs for energy supplied to the grid ($0.1700/kWh for peak {equivalent to 65 Baiza} and $0.0310/kWh for off-peak {equivalent to 12 Baiza}) according to a report published on *12th June, 2017, in Times of OMAN* electric subsidy in Oman and also acknowledges daylight saving time changes, starting in March for summer and October for winter. The accompanying doughnut chart illustrates the peak (07:00-20:00) and off-peak (20:00-07:00) hours for the tariff application.

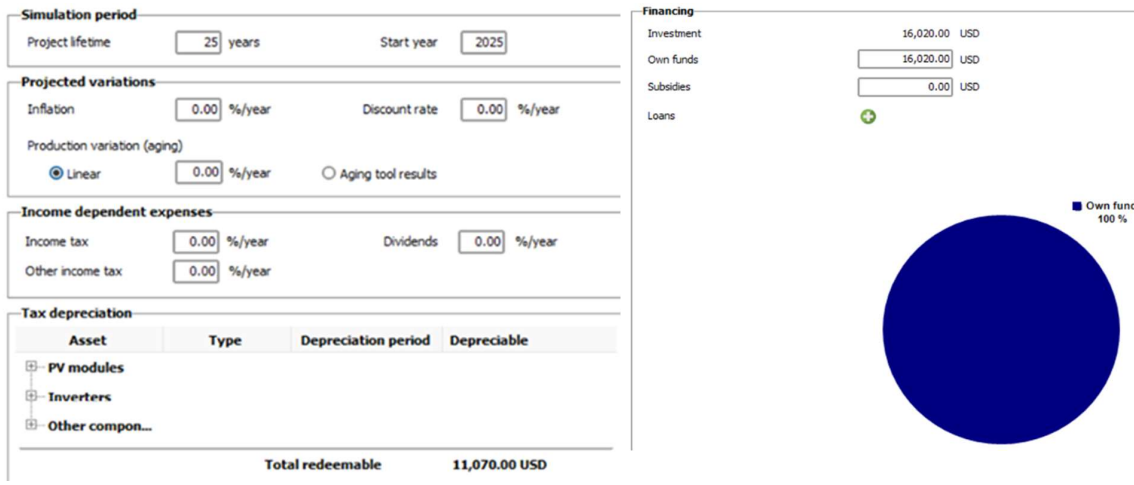

Fig. 14: Financial model overview for a 25-year project, fully self-funded.

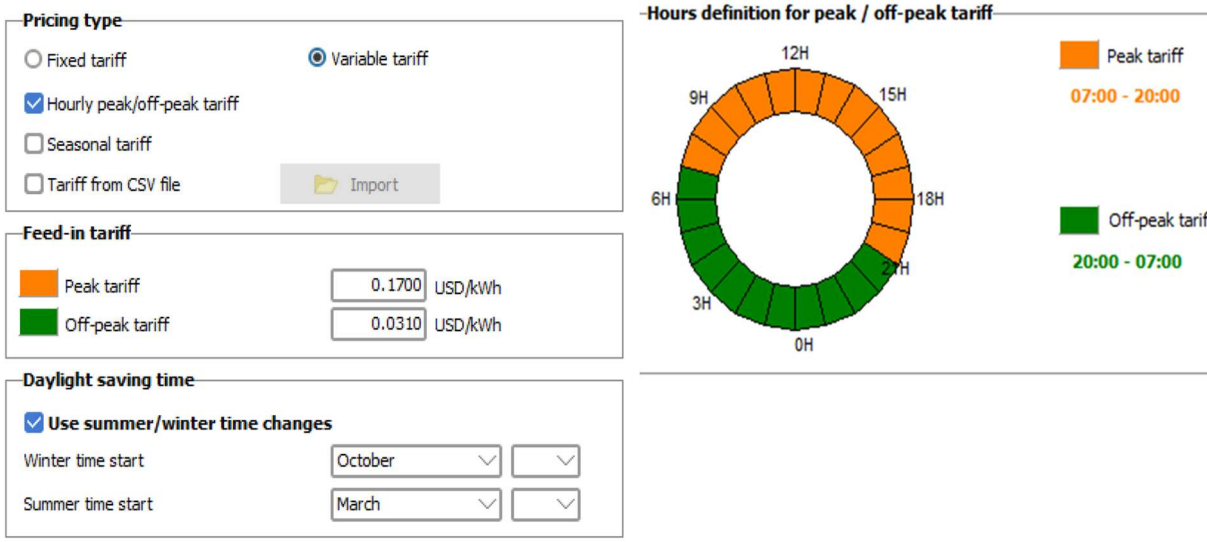

Fig. 15: Variable energy pricing model with peak and off-peak hours.

Financial result: The total installation cost for the PV system is $ 16,020.00, which is fully funded by the owner without subsidies or loans. The system has a depreciable asset value of $11,070.00 and yearly operating costs of $1,040.00 to $1,250.00. Financially, the system's NPV is $32,024.28 with an 11.15% Internal Rate of Return (IRR), and the payback period is 7.5 to 8.3 years. The Levelized Cost of Energy (LCOE) is $0.1013/kWh, and the Return on Investment (ROI) is 232.7%. PV modules constitute roughly 57.07% of the capital costs, and other components total $1,600.00. O&M practices like biweekly cleaning of PV modules are crucial for system upkeep. Financial metrics indicate that the investment would be recoverable in about 7.5 years, assuming stable performance and savings as shown in Fig. 16.

Solar project financial forecast: Fig. 17 (a) illustrates the annual cash flow for a solar project in USD, starting with a significant initial investment depicted by a large red bar exceeding $16,000, followed by annual net incomes shown as green bars. Each subsequent year reflects profitable operations with these green bars, indicating consistent yearly earnings in the thousands. Fig. 17 (b) portrays the cumulative cash flow, beginning with the initial outlay and tracing the transition to profitability. This chart gradually transforms from red to green as the project moves toward and surpass-

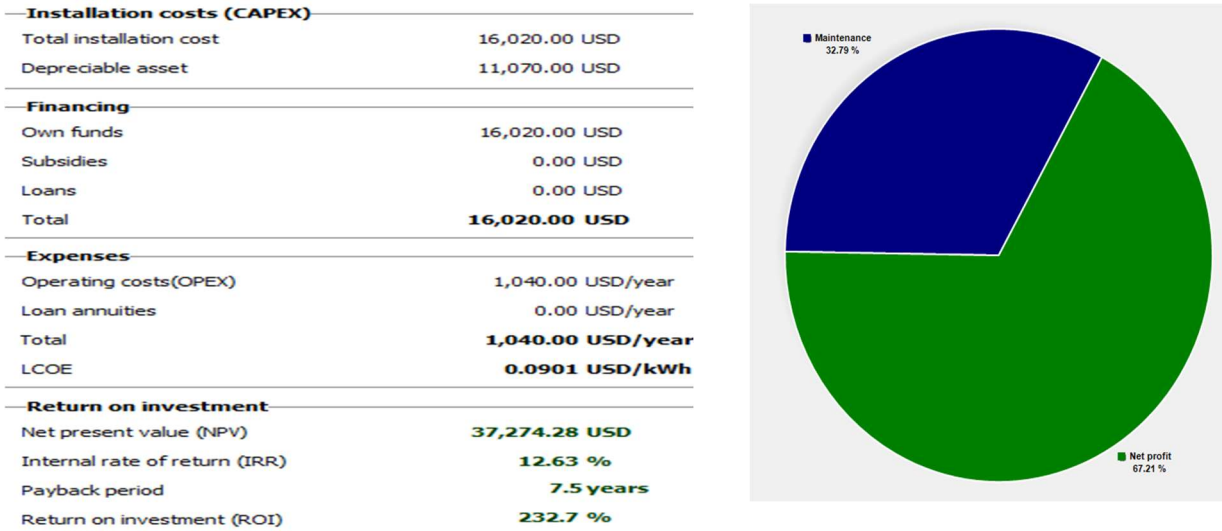

Fig. 16: Project financial summary: costs, funding, returns, and profit distribution.

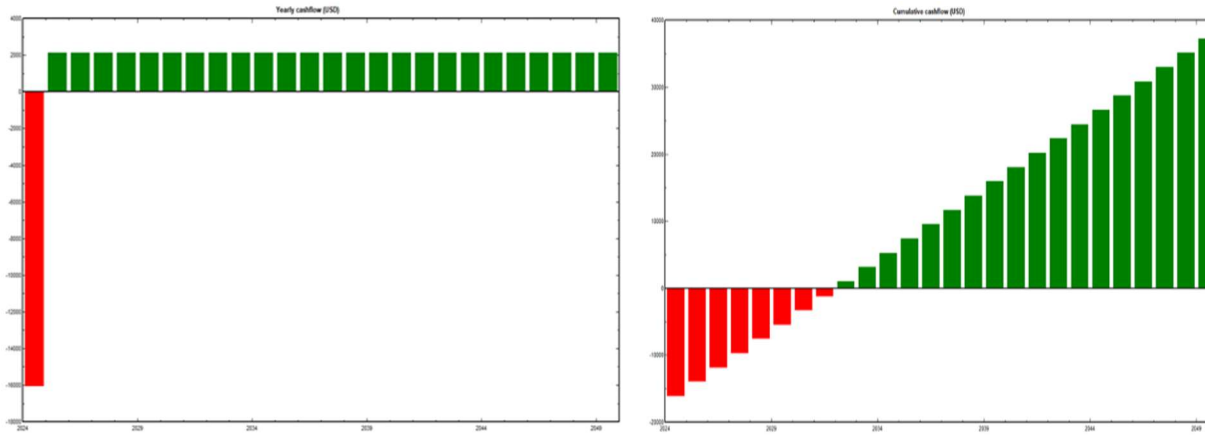

Fig. 17: (a) Yearly net loss and profit; (b) Economic feasibility.

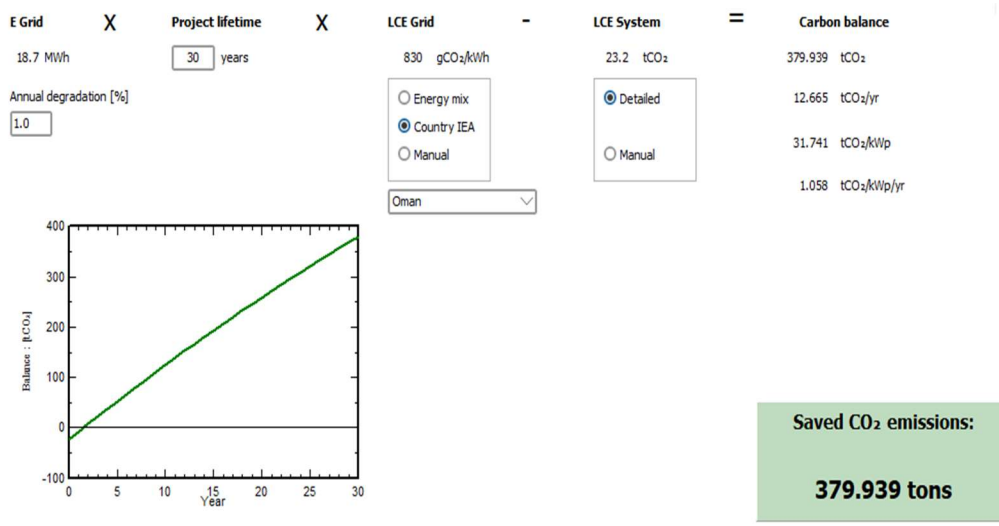

Fig. 18:Environmental impact of a 30-year solar project.

es the break-even point. Numerically, the cumulative cash flow, starting with the initial investment, reaches a positive territory exceeding $30,000 after several years, effectively visualizing the payback period and subsequent profitability for stakeholders. These visual aids are crucial for illustrating the timeline for the investment's return and ongoing financial benefits.

CO_2 Emission Balance

Fig. 18, presents data related to the environmental impact over the project's lifetime, set at 30 years. The grid electricity (E Grid) produced by the system is 18.7 MWh, and the system experiences a 1% annual degradation in performance. The carbon emissions factor for grid electricity (LCE Grid) in Oman is 830 gCO_2/kWh, whereas the system's emissions factor (LCE System) is significantly lower at 23.2 tCO_2. It is likely to illustrate the cumulative carbon savings over the project's lifetime, indicating a linear increase in carbon savings as the project continues to operate. The "Carbon balance" section quantifies the total CO_2 savings at 379.939 tons over the project's lifetime. This breaks down to 12.665 tCO_2/year, and when normalized to the system production, it is 31.741 tCO_2/kWp or 1.058 tCO_2/kWp/year. The highlight of this analysis is the "Saved CO_2 emissions," which stands at 379.939 tons, showcasing the project's substantial environmental benefits by reducing carbon emissions compared to conventional grid energy sources.

CONCLUSION

This study examined the feasibility, methods, and key findings of a grid-connected PV system designed for a building in Ibri, Oman. The system, proposed to be 10.81

kWp, focused on cost efficiency, surplus energy utilization, and minimizing the carbon footprint. The system components included PV panels, inverters, and charge controllers, with a detailed comparison of panel types based on material composition, efficiency, costs, and applications. The PVsyst software was employed for design and simulation, considering local climate conditions and solar orientation to maximize efficiency. Key performance metrics such as the performance ratio (PR), capacity utilization factor, and system efficiency were evaluated to determine the system's effectiveness. The study emphasized the importance of these parameters in optimizing the design and performance.

The findings indicated that the PV system generated 16,981 kWh annually, with a yield of 1,419 kWh/kWp and a PR of 0.672, demonstrating efficient sunlight conversion. The in-depth evaluations of energy generation and efficiency measures highlighted the need to minimize losses. Financial analysis demonstrated a payback period of 7.5 to 8.3 years, with an IRR of 11.15% and an NPV of $32,024.28, proving economic viability. The project also predicted a reduction of 379.939 tons of CO_2 over its lifespan, showcasing significant environmental benefits. The comprehensive examination of design, simulation, installation, and performance confirmed that the system was technically feasible, financially viable, and environmentally beneficial. This study offers a valuable understanding of similar geographic and climatic conditions, guiding future projects toward achieving positive outcomes.

NOMENCLATURE

Latin Symbols			
V	Voltage	BIM	Building information model
KWh	Kilowatt-hour	IPPs	Independent power projects
tCO_2	Metric tons of CO2	STC	Standard test conditions
KWp	Kilowatt peak	PR	Performance ratio
$	US Dollar	CO_2	Carbon dioxide
P_T	Rated power	GIS	Geographic information system
P_D	Total power	LCE	Life cycle emission
E_T	Total energy	AC	Alternating current
E_g	Gross energy	DC	Direct current
		I-V	Current (I) versus Voltage (V)

Greek Symbols			
a	Tilt angle	DOD	MPP
b	Azimuth angle	NPV	Net present value
		IAM	Incidence angle modifier

Abbreviation	
PV	Photovoltaic
SE	Solar energy
IEA	International energy agency
PVsyst	Photovoltaic system (software)

REFERENCES

Al-Badi, A., Malik, A., Al-Areimi, K. and Al-Mamari, A., 2009. Power sector of Oman-Today and tomorrow. *Renewable and Sustainable Energy Reviews*, 13(8), pp.2192–96. doi:10.1016/j.rser.2009.03.010.

Albadi, M.H., Al-Hinai, A.S., Al Maharbi, M.J., Al Hosni, A.M. and Al Hajri, M.A., 2019. Economic dispatch of Oman's main interconnected system in presence of 500MW solar PV plant in Ibri. *2019 IEEE Jordan International Joint Conference on Electrical Engineering and Information Technology (JEEIT 2019) Proceedings*, pp.204–08. doi:10.1109/JEEIT.2019.8717418.

Alimi, O.A., Meyer, E.L. and Olayiwola, O.I., 2022. Solar photovoltaic modules' performance reliability and degradation analysis-A review. *Energies*, 15(16), 5964. doi:10.3390/en15165964.

Bagwari, A., Samarah, A., Gangwar, R.P.S., Anandaram, H., Elkady, G., Al Ansari, M.S., Arya, G. and Uniyal, J., 2022. Solar energy technology: Step towards a bright future of the world. *International Journal of Mathematical, Engineering and Management Sciences*, 7(6), pp.982–1004. doi:10.33889/IJMEMS.2022.7.6.061.

Charabi, Y., 2023. Status and future prospects of wind energy in Oman. *Springer*. doi:10.1007/698_2022_959.

Coyle, E., 2017. A case study of the Omani electricity network and readiness for solar energy integration. *SDAR Journal of Sustainable Design & Applied Research*, 5(1), pp.1-10.

Emerald Insight, 2022. Oman's green hydrogen sector will grow over the decade. *Emerald*. Available at: https://www.emerald.com/insight/content/doi/10.1108/OXAN-DB273230/full/html

Gastli, A. and Charabi, Y., 2010. Solar electricity prospects in Oman using GIS-based solar radiation maps. *Renewable and Sustainable Energy Reviews*, 14(2), pp.790–97. doi:10.1016/j.rser.2009.08.018.

Guo, F., Gao, J., Men, H., Fan, Y. and Liu, H., 2021. Large-scale group decision-making framework for the site selection of integrated floating photovoltaic-pumped storage power system. *Journal of Energy Storage*, 43, 103125. doi:10.1016/j.est.2021.103125.

Kazem, H.A., Albadi, M.H., Al-Waeli, A.H.A., Al-Busaidi, A.H. and Chaichan, M.T., 2017. Techno-economic feasibility analysis of 1MW photovoltaic grid-connected system in Oman. *Case Studies in Thermal Engineering*, 10, pp.131–41. doi:10.1016/j.csite.2017.05.008.

Kim, G.G., Hyun, J.H., Choi, J.H., Ahn, S.H., Bhang, B.G. and Ahn, H.K., 2023. Quality analysis of photovoltaic system using descriptive statistics of power performance index. *IEEE Access*, 11, pp.28427–38. doi:10.1109/ACCESS.2023.3257373.

Lee, A.H.I., Kang, H.Y., Lin, C.Y. and Shen, K.C., 2015. An integrated decision-making model for the location of a PV solar plant. *Sustainability*, 7(10), pp.13522–41. doi:10.3390/su71013522.

Maran, K., Senthilnathan, C.R., Usha, S. and Venkatesh, P., 2022. Impact of solar energy on mitigating climate changes for a sustainable

development in India. *Proceedings of the 3rd International Conference on Power, Energy, Control and Transmission Systems (ICPECTS 2022)*. doi:10.1109/ICPECTS56089.2022.10046744.

Mukhopadhyay, S., 2022. Solar energy and gasification of MSW: Two promising green energy options. *Green Energy Systems: Design, Modelling, Synthesis and Applications*, pp.93–125. doi:10.1016/B978-0-323-95108-1.00003-3.

Munshi, A.A., 2023. Evaluation of grid-connected photovoltaic plants based on clustering methods. *Computer Systems Science and Engineering*, 45(3), pp.2837–52. doi:10.32604/csse.2023.033168.

Nayak, M.R., Srikanth, Y., Padmavathi, M. and Khasim, S.R., 2022. Enhancement of solar PV cell efficiency using instantaneous light reflection technique. *Proceedings of the International Conference on Computational Intelligence and Sustainable Engineering Solutions (CISES 2022)*, pp.202–8. doi:10.1109/CISES54857.2022.9844402.

Ninzo, T., Mohammed, J.M. and Venkateswara, R.C., 2023. Enactment of NZEB by state of art techniques in Sultanate of Oman. *i-manager's Journal on Future Engineering and Technology*, 18(3), pp.1-9. doi:10.26634/jfet.18.3.19163.

Peters, I.M. and Sinha, P., 2021. Value of stability in photovoltaic life cycles. *Conference Record of the IEEE Photovoltaic Specialists Conference*, pp.416–19. doi:10.1109/PVSC43889.2021.9518480.

Qingyang, J., Jichun, Y., Yanying, Z. and Huide, F., 2021. Energy and exergy analyses of PV, solar thermal and photovoltaic/thermal systems: A comparison study. *International Journal of Low-Carbon Technologies*, 16(2), pp.604–11. doi:10.1093/ijlct/ctaa092.

Rahman, T., Al Mansur, A., Hossain Lipu, M.S., Rahman, M.S., Ashique, R.H., Abou Houran, M., Elavarasan, R.M. and Hossain, E., 2023. Investigation of degradation of solar photovoltaics: A review of aging factors, impacts, and future directions toward sustainable energy management. *Energies*, 16(9), 3706. doi:10.3390/en16093706.

Sheikholeslami, M., 2023. Nanotechnology applications for solar energy systems. *Nanotechnology Applications for Solar Energy Systems*, pp.1-430. doi:10.1002/9781119791232.

Shekhar, R., 2018. Innovative uses of solar thermal technology. In: *Renewable Energy and Green Technology*. pp.3–9. doi:10.1007/978-981-10-4576-9_1.

Tabook, M. and Khan, S.A., 2021. The future of the renewable energy in Oman: Case study of Salalah City. *International Journal of Energy Economics and Policy*, 11(6), pp.517–22. doi:10.32479/ijeep.11855.

Xu, X., Wu, W. and Wang, Q., 2023. Efficiency improvement of industrial silicon solar cells by the POCl3 diffusion process. *Materials*, 16(5), 1824. doi:10.3390/ma16051824.

Yamaguchi, M., Masuda, T., Nakado, T., Yamada, K., Okumura, K., Satou, A., Ota, Y., Araki, K. and Nishioka, N., 2022. Analysis for solar coverage and CO_2 emission reduction of photovoltaic-powered vehicles. *IEEE Photovoltaic Specialists Conference*, pp.58–58. doi:10.1109/pvsc48317.2022.9938513.

Yousefi, H., Hafeznia, H. and Yousefi-Sahzabi, A., 2018. Spatial site selection for solar power plants using a GIS-based Boolean-fuzzy logic model: A case study of Markazi Province, Iran. *Energies*, 11(7), 1648. doi:10.3390/en11071648.

Zurigat, Y.H., Sawaqed, N.M., Al-Hinai, H. and Jubran, B.A., 2007. Analysis of typical meteorological year for Seeb/Muscat, Oman. *International Journal of Low Carbon Technologies*, 2(4), pp.323–38. doi:10.1093/ijlct/ctm027.

ORCID DETAILS OF THE AUTHORS

Arshad Mehmood: https://orcid.org/0009-0004-0750-3150